Journal of Chemical and Petroleum Engineering 2020, 54(1): 35-46
DOI: 10.22059/jchpe.2019.281905.1278

RESEARCH PAPER

Oil Refinery Wastewater Treatment by Advanced Oxidation Processes for Chemical Oxygen Demand Removal using the Box-Behnken Method

Majid Mohadesi, Babak Aghel*, Mohammad Hamed Razmegir, Ashkan Gouran

Department of Chemical Engineering, Faculty of Energy, Kermanshah University of Technology, Kermanshah, Iran

Received: 22 May 2019, Revised: 13 August 2019, Accepted: 21 October 2019

Abstract

This study investigated the reduction of the chemical oxygen demand from the Kermanshah oil refinery wastewater using Fenton and Photo-Fenton processes. The study investigated the effects of operating variables such as ultraviolet light intensity in values of 0, 15, and 30 W, ferrous ion concentration in values of 10, 50, and 90 mg/l, hydrogen peroxide concentration in values of 100, 500 and, 900 mg/l, and treatment time in values of 30, 90, and 150 min on the reduction of the chemical oxygen demand percentage from this industrial wastewater. All the experiments were carried out in a glass reactor at a temperature of 25 ℃ under a stirrer speed of 350 rpm. Using the Box-Behnken experimental method, 27 experiments were performed randomly. Then, using the least-squares error method, an experimental quadratic model was achieved. Analysis of variance of the model showed that the proposed model had a high level of accuracy. Finally, we obtained the optimum conditions for maximizing the percentage of the chemical oxygen demand removal from the wastewater. The optimal conditions were Fe^{2+} concentration of 89.2 mg/l, H2O2 concentration of 119.9 mg/l, and treatment time of 135.9 min for the Fenton process. Also, these conditions were Fe^{2+} concentration of 35.1 mg/l, H_2O_2 concentration of 110.2 mg/l, treatment time of 92.8 min, and ultraviolet light intensity of 30 W, for the photo-Fenton process. Under these conditions, the percentage of chemical oxygen demand removal using the proposed model was 96.61 % and 92.82 % for the Fenton and photo-Fenton processes, respectively.

Keywords:
COD Removal,
Design of Experiment,
Fenton Process,
Industrial Wastewater Treatment,
Photo-Fenton Process

Introduction

Over the last decades, there has been considerable progress in the advanced oxidation process (AOP) and it has been recognized as an important process for the treatment of industrial wastewater, especially those containing organic materials that reduce water quality and cannot be treated via conventional purification methods. In general, advanced oxidation processes includes all the processes in which active hydroxyl radicals (OH^*) are produced in various ways. Because of the high oxidation capacity of the radical hydroxyl (2.8 volts), the majority of advanced oxidation processes are performed through the production of this active radical [1-3].

The UV/H_2O_2 process is a type of advanced oxidation process and a treatment method that has significantly progressed over the last decade. The literature has proposed different mechanisms for the UV/H_2O_2 photo-oxidation process. This method is very effective in the removal of organic contaminants and in controlling the parameters reducing the quality of water

* Corresponding author:
Email: babakaghel@gmail.com (B. Aghel)

such as dissolved oxygen (DO), biological oxygen demand (BOD), and chemical oxygen demand (COD). Nowadays, there is an accepted mechanism in which hydroxyl radicals are produced by exposing a solution containing H_2O_2 to UV light. In the Fenton process, iron salts are added to H_2O_2 and hydroxyl radicals are produced as presented in the following formula.

$$Fe^{2+} + H_2O_2 \rightarrow Fe^{3+} + OH^{\bullet} + OH^{-} \quad (k = 76\ \frac{mol}{l.s}) \tag{1}$$

$$Fe^{3+} + H_2O_2 \rightarrow Fe^{2+} + HO_2^{\bullet} + H^{+} \quad (k = 0.02\ \frac{mol}{l.s}) \tag{2}$$

To enhance the Fenton reaction, photo-Fenton is introduced by the UV light. When ultraviolet radiation is applied, Fe^{2+} is reproduced as presented in the following formula.

$$Fe(OH)^{2+} + h\nu \rightarrow Fe^{2+} + OH^{\bullet} \tag{3}$$

$$Fe(H_2O)_6{}^{3+} + h\nu \rightarrow Fe^{2+} + OH^{\bullet} + H^{+} \tag{4}$$

The reduction of Fe^{3+} to Fe^{2+} is an advantage because there is no further need to continuously add Fe^{2+} in the Fenton reaction. Moreover, the two abovementioned reactions reproduce hydroxyl radicals. In addition, hydrogen peroxide under the ultraviolet light produces two radical hydroxyls that act as strong oxidant agents [4-7].

$$H_2O_2 + h\nu \rightarrow 2OH^{\bullet} \tag{5}$$

Meric et al. [8] studied the wastewater containing Reactive Black 5 (RB 5); they used the Fenton method and studied different H_2O_2 and $FeSO_4$ concentrations, pH, and temperature as process parameters of the Fenton process, and finally, they achieved a COD removal rate of 84% and a color removal rate of more than 99%. Arslan-Alaton et al. [9] investigated parameters such as the concentration of H_2O_2 and Fe^{3+}, reaction time, and the baseline COD of colored wastewater containing AB193. Using the photo-Fenton, they reduced the color of the wastewater, COD, and TOC by 98%, 78%, and 59%, respectively. Hasan et al. [10] investigated the effects of the photo-Fenton process on the refinery wastewater and reported COD and TOC removal rates of 98% and 70%, respectively, at a pH of 3, during a time of 30 min, with optimal concentrations of Fenton reactants. Hermosilla et al. [11] used photo-Fenton and Fenton processes and removed the COD and TCO by up to 70%, and also found that photo-Fenton used iron 32 times less than Fenton process and it reduced the production of sludge by 25 times.

There are two main types of response surface designs (RSM) named central composite design and Box-Behnken design. The central composite design is the most generally used as a fractional factorial design with center points but in the Box-Behnken design. It does not contain an embedded fractional factorial design. So, since there are more points in the middle of the range the Box Behnken may seem more desirable. Box-Behnken designs typically have fewer points than central composite designs and efficiently estimate the first- and second-order coefficients to fit a full quadratic model [12]. Among all other response surface methodology designs, Box-Behnken experimental designs need fewer runs (27 runs for 4 factors) [13].

In this study, Kermanshah oil refinery wastewater was treated using Fenton and photo-Fenton processes. In order to reduce the COD from this industrial wastewater, we investigated the effects of different variables. This study investigated the effect of UV light intensity, ferrous concentration, hydrogen peroxide concentration, and treatment time on the COD removal using Box-Behnken experimental design.

Materials and Methods

Materials

The wastewater of the Kermanshah oil refinery plant was treated in this study. Table 1 shows the physicochemical characteristics of the Kermanshah oil refinery wastewater, including total suspended solids (TSS), total dissolved solids (TDS), BOD, COD, and turbidity. Iron (II) sulfate heptahydrate ($FeSO_4.7H_2O$) as the source of Fe^{2+}, hydrogen peroxide solution (30% w/w), and MnO_2 were obtained from Merck. Deionized water was used in all the experiments.

Table 1. Physio-chemical characteristics of the Kermanshah oil refinery wastewater

Property	Unit	Results
TDS	mg/l	960
TSS	mg/l	186
BOD	mg/l	45
COD	mg/l	368
Turbidity	NTU	63

The procedure of the experiments

The experiments were carried out in a glass container with a volume of 1 liter. Two Phillips mercury lamps 15 watts (UV-C) that were placed horizontally at top of the reactor (inside a dark box) were used as the source of the light. All the experiments were carried out at a temperature of 25 °C, atmospheric pressure, and under a stirring speed of 350 rpm (in order to prevent iron ion sedimentation and to keep the mixture homogenized). The schematic of the set-up used in this study is shown in Fig. 1. After testing, the COD content of the samples was measured using a spectrophotometer (DR 5000, Hach, Jenway, USA) at 600 nm.

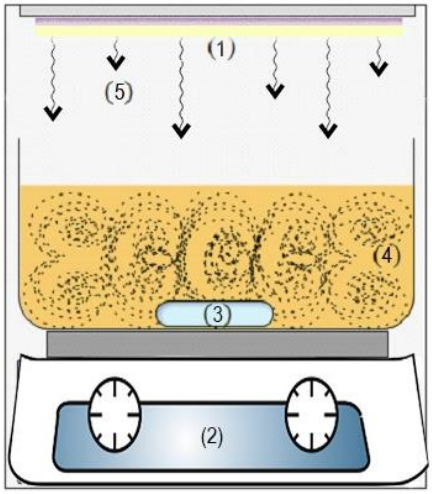

Fig. 1. Schematic diagram of the setup. (1) UV lamp, (2) Magnetic stirrer, (3) Magnetic stirrer bar (4) Glass reactor, and (5) Dark box

Each experiment was conducted on 500 ml of industrial wastewater. The effects of different concentrations of H_2O_2 and Fe^{2+}, treatment time, and UV light intensity on the percentage of the COD removal were studied. The COD was measured in keeping with the standard methods [14]. The COD removal percent was calculated as follows:

$$\text{COD removal } (\%) = \left(\frac{[COD]_0 - [COD]}{[COD]_0}\right) \times 100 \quad (6)$$

where $[COD]_0$ is COD value at the start of the reaction (COD of the refinery wastewater) and $[COD]$ is the COD value at the time of the process (t).

The remaining amount of the hydrogen peroxide in samples interfered with the COD test and was removed by MnO_2 and then to separate MnO_2 powder the samples were filtered [15].

Design of experiments and statistical analysis

This study used the experimental design method and the COD removal percent as the response was investigated to determine the optimal conditions. For the optimization of the process, the variables of UV intensity, Fe^{2+} concentration, H_2O_2 concentration, and treatment time were evaluated. Table 2 presents input variables (UV, $[Fe^{2+}]$, $[H_2O_2]$, and t), and levels.

Table 2. Operation parameters and their levels

Factor	Unit	Symbol	Levels		
			Low	Middle	High
Ultraviolet intensity	W	UV	0	15	30
Ferrous concentration	mg/l	$[Fe^{2+}]$	10	50	90
Hydrogen peroxide concentration	mg/l	$[H_2O_2]$	100	500	900
Treatment time	min	t	30	90	150

The Box-Behnken design among all the RSM with the same number of factors requires a fewer number of experiments [16]. Taking into account the design of the experiments, the following model for the response variable (*Res.*) was presented as a polynomial equation:

$$Res. = b_0 + \sum b_i x_i + \sum\sum b_{ij} x_i x_j + \sum\sum b_{ii} x_i^2 + \varepsilon \quad (7)$$

where b_0 is a constant number, ε is the residual of the equation, b_{ij} is a linear interaction between the input variables x_i and x_j (i= 1, 2, 3 and j= 1, 2, 3, 4), b_j is the slope of the variable, b_{ii} is the second-order of the input variable x_i (i= 1, 2, 3, 4). Moreover, the significance of each variable in the polynomial equation (Eq. 7) was examined by analysis of variance (ANOVA) [16].

According to the analysis of variance, the p-value or significance level was set at 0.05. Also, the statistical significance of models was determined using the F-value. When the calculated F-value is larger than the tabulated F-value, the p-value will be much smaller; this fact indicates the significance of the statistical model. The calculated F-value was calculated by dividing the regression mean square into the residual mean square, as follows [17]:

$$F - \text{value} = \frac{MS_{\text{regression}}}{MS_{\text{residual}}} \quad (8)$$

where

$$MS_{\text{regression}} = \frac{SS_{\text{regression}}}{DF_{\text{regression}}} \quad (9)$$

$$MS_{\text{residual}} = \frac{SS_{\text{residual}}}{DF_{\text{residual}}} \quad (10)$$

Regression degree of freedom ($DF_{\text{regression}}$) is the number of sentences minus one and the residual degrees of freedom (DF_{residual}) is the total degrees of freedom minus the regression degree of freedom [17]. Table 3 presents the experimental design that was consisted of 27 tests and the percentages of COD removal. It should be noted that in order to minimize the experimental errors all the experiments were randomly carried out.

Table 3. Designing experiments using the Box–Behnken method and response

	Manipulated variables				Response
No.	***UV*, W**	**$[Fe^{2+}]$, mg/l**	**$[H_2O_2]$, mg/l**	***t*, min**	**COD removal, %**
1	30	50	900	90	77.65
2	15	10	900	90	69.50
3	15	50	900	30	76.74
4	15	50	100	30	47.78
5	30	50	100	90	83.98
6	0	50	900	90	87.60
7	15	10	100	90	55.93
8	30	90	500	90	76.74
9	30	50	500	30	75.84
10	15	10	500	30	32.40
11	15	90	900	90	76.74
12	15	50	500	90	71.31
13	15	50	900	150	28.69
14	15	50	500	90	62.26
15	0	90	500	90	87.60
16	30	50	500	150	48.69
17	0	50	500	150	55.93
18	15	10	500	150	58.55
19	0	50	100	90	65.88
20	30	10	500	90	85.79
21	15	90	500	150	61.36
22	15	50	100	150	83.08
23	15	50	500	90	75.84
24	15	90	100	90	77.65
25	0	10	500	90	26.06
26	0	50	500	30	40.54
27	15	90	500	30	55.93

Results and discussion

Experimental design and ANOVA of response

The main objective of this part of the study was to determine the optimum conditions for obtaining the maximum percentage of COD removal in the Fenton and photo-Fenton processes. In this study, the effects of the four independent variables (UV intensity, Fe^{2+} concentration, H_2O_2 concentration and treatment time) on the response function ($COD_{rem.}$) were investigated using the Box-Behnken design. Table 3 presents the experimental results and the obtained percentages of the COD removal. The quadratic relations were obtained using the least-squares error method, for determining the response in terms of the four variables, as follows:

$$COD_{rem.} = -81.227 + 3.244UV + 1.185[Fe^{2+}] + 0.076[H_2O_2] + 1.516t - 0.029UV.[Fe^{2+}] - 1.169 \times 10^{-3}UV.[H_2O_2] - 0.012UV.t - 2.262 \times 10^{-4}[Fe^{2+}].[H_2O_2] - 2.158 \times 10^{-3}[Fe^{2+}].t - 8.682 \times 10^{-4}[H_2O_2].t + 0.012UV^2 - 2.123 \times 10^{-3}[Fe^{2+}]^2 + 3.108 \times 10^{-5}[H_2O_2]^2 - 4.371 \times 10^{-3}t^2 \quad (11)$$

The predicted values of the quadratic Eq. 11 were compared with the observed value and were shown in Fig. 2.

Table 4 presents the results ANOVA which was performed to evaluate the model developed for assessing the COD removal percentage. According to Table 4, the total degree of freedom was 26, and degrees of freedom for the model and the residual error were 14 and 12, respectively. Moreover, since the tabulated F-value was lower than the calculated F-value; consequently, the p-value was low (*p*-value = 0.0014) and the model was statistically significant. The terms of $[Fe^{2+}]$, $UV.[Fe^{2+}]$, $[H_2O_2].t$, and t^2 had a *p*-value of less than 0.01 and

were statistically significant. Furthermore, *UV* and *UV.t* had 0.01<*p*-value<0.05 and they were also significant terms [17]. Although the terms of [H_2O_2] and *t* were related to independent variables and were insignificant, the interaction between these parameters ([H_2O_2].t) and *UV.t* was significant. Further, the *p*-value for *Lack of Fit* was higher than 0.05 that was representative of the match of the presented model.

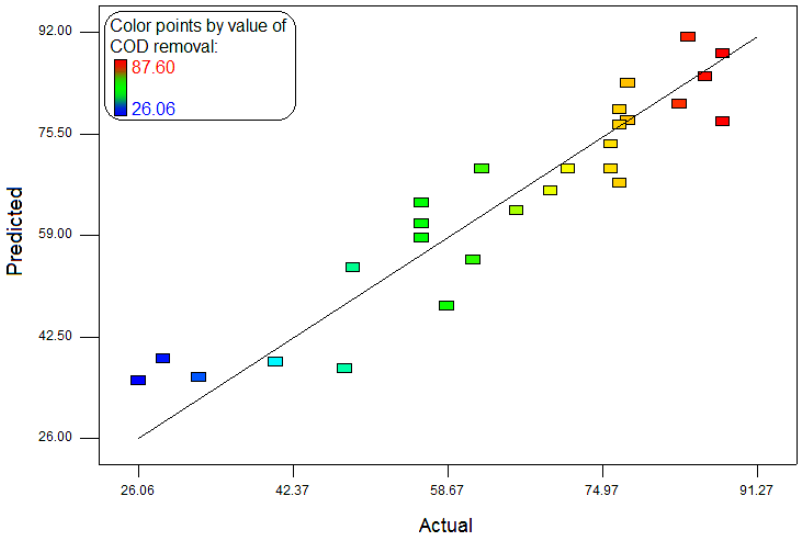

Fig. 2. Comparison between the actual and predicted values of the COD removal (at a temperature of 25 °C, atmospheric pressure and under a stirring speed of 350 rpm)

Table 4. Analysis of variance (ANOVA) of the quadratic model of the percentage of the COD removal

Source	Sum of Squares	DF	Mean Square	*F*-Value	*p*-Value Prob > *F*	Level of Significance
Model	7515.42	14	536.82	6.32	0.0014	highly significant
UV	603.08	1	603.08	7.10	0.0206	Significant
$[Fe^{2+}]$	968.22	1	968.22	11.40	0.0055	highly significant
$[H_2O_2]$	0.57	1	0.57	6.684×10^{-3}	0.9362	not significant
t	4.17	1	4.17	0.049	0.8285	not significant
$UV.[Fe^{2+}]$	1245.74	1	1245.74	14.67	0.0024	highly significant
$UV.[H_2O_2]$	196.84	1	196.84	2.32	0.1538	not significant
$UV.t$	452.41	1	452.41	5.33	0.0396	significant
$[Fe^{2+}].[H_2O_2]$	52.42	1	52.42	0.62	0.4473	not significant
$[Fe^{2+}].t$	107.33	1	107.33	1.26	0.2829	not significant
$[H_2O_2].t$	1736.81	1	1736.81	20.45	0.0007	highly significant
UV^2	36.27	1	36.27	0.43	0.5257	not significant
$[Fe^{2+}]^2$	61.55	1	61.55	0.72	0.4113	not significant
$[H_2O_2]^2$	131.89	1	131.89	1.55	0.2365	not significant
t^2	1320.83	1	1320.83	15.55	0.0019	highly significant
Residual	1019.10	12	84.93			
Lack of Fit	923.49	10	92.35	1.93	0.3890	not significant
Pure Error	95.61	2	47.81			
Cor Total	8534.52	26				

Effect of operational variables

As mentioned, we investigated the effects of UV intensities of 0, 15, and 30 watts, Fe (II) concentration of 10, 50, and 90 mg/l, H_2O_2 the concentration of 100, 500, and 900 mg/l, and the treatment times of 30, 90, and 150 min on the COD removal. The three-dimensional plots of COD removal versus different variables using Eq. 11 were shown in Figs. 3 to 8.

Fig. 3 shows the COD removal by the UV intensity and Fe^{2+} concentration when using $[H_2O_2] = 500$ mg/l with a time of $t = 90$ min. It was observed that at low concentrations of Fe^{2+} ($[Fe^{2+}] = 10$ mg/l), when the UV intensity was at its pick ($UV = 30$ W), the maximum COD removal was achieved. Moreover, when using $[Fe^{2+}] = 90$ mg/l, the maximum COD removal rate was achieved when the UV lamps were off ($UV = 0$ W). In other words, the use of high concentrations of iron ion in the Fenton process and low concentrations of Fe (II) in the photo-Fenton process resulted in a higher COD removal rate. It is known that with increasing iron ion concentration, the COD removal rate in the Fenton process increases, as presented by Eqs. 12 and 13, respectively.

$$H_2O_2 + Fe^{+2} \rightarrow OH^{\bullet} + OH^{-} + Fe^{+3} \quad (12)$$

$$OH^{\bullet} + Fe^{+2} \rightarrow OH^{-} + Fe^{+3} \quad (13)$$

In the Fenton process, with an increase in Fe^{2+} concentration from 10 to 90 mg/l, there was an increase in the production of hydroxyl radicals that was followed by the removal of the COD. However, with increasing iron ion concentration in the photo-Fenton process, the COD removal rate decreased, because, at high concentrations of iron ion, the initial production rate of hydroxyl radicals, which is mainly formed by H_2O_2 decomposition is very high. Therefore, many hydroxyl radicals are consumed by side reactions, before they are consumed for the COD removal [18] (Eq. 5). Additionally, high concentrations of Fe (II) can cause brown turbidity. Therefore, the absorption of UV light which is required for photolysis was delayed and the recombination of OH^{*} radicals occurred (see Eq. 3). This finding has been also reported by many other researchers [19,20].

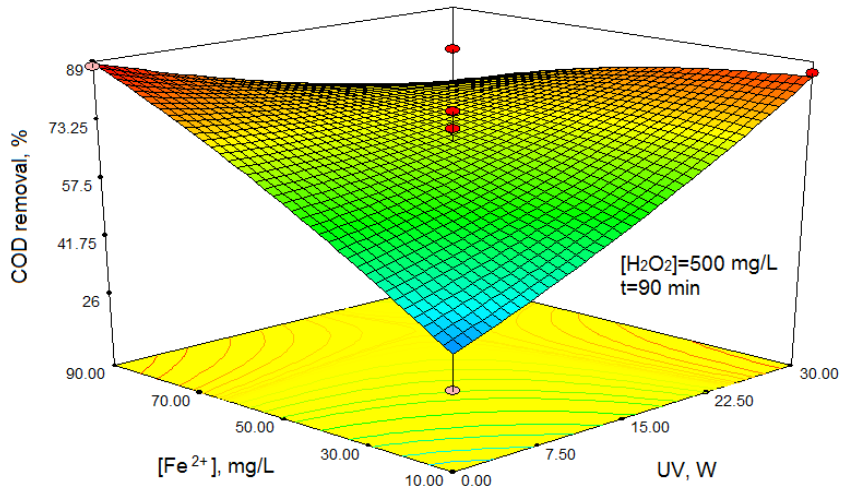

Fig. 3. Three-dimensional plot of the COD removal by ultraviolet intensity and ferrous concentration ($[H_2O_2] = 500$ mg/l, $t = 90$ min, $T = 25$ ℃, $P = 1$ atm, and stirring speed of 350 rpm)

Fig. 4 shows a three-dimensional plot of the COD removal by UV intensity and H_2O_2 concentration when using $[Fe^{2+}] = 50$ mg/l with a time of $t = 90$ min. As shown in this figure, using a low concentration of H_2O_2 ($[H_2O_2] = 100$ mg/l) when the intensity of the UV light is 30 W, the COD removal was at the highest level. Moreover, when using higher concentrations of H_2O_2 under lower levels of UV light intensity, the COD removal rate was better. On the other hand, with increasing concentrations of H_2O_2 in the Fenton process ($UV = 0$ W), the COD removal rate increased. In addition, in a moderate UV light intensity ($UV = 15$ W), variations in hydrogen peroxide concentration had a small effect on the COD removal rate.

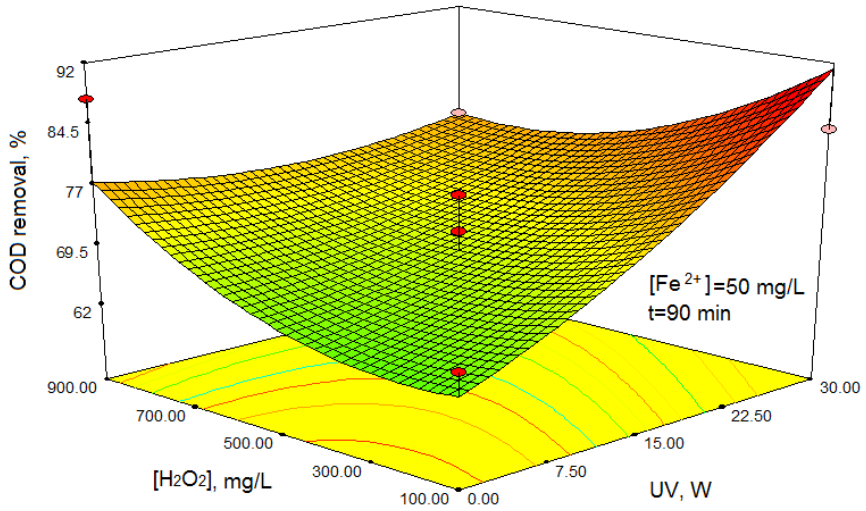

Fig. 4. Three-dimensional plot of the COD removal by ultraviolet intensity and hydrogen peroxide concentration ($[Fe^{2+}] = 50$ mg/l, $t = 90$ min, $T = 25$ ℃, $P = 1$ atm, and stirring speed of 350 rpm)

Fig. 5 shows a three-dimensional plot of the COD removal by UV intensity and treatment time when using $[Fe^{2+}] = 50$ mg/l and $[H_2O_2] = 500$ mg/l. As shown in this figure, the photo-Fenton process with a UV intensity of 30 W had a higher COD removal rate than the Fenton process (UV = 0 W). Moreover, during the average treatment time, the COD removal rate was higher than the rate observed over all other times at all UV light intensity values. It might be justified by the formation of by-products over time, as no further COD reduction occurs over time [18]. In addition, at a higher UV intensity, less time is needed to remove COD. In other words, the maximum amount of COD removal occurs at a higher UV intensity during shorter treatment time. These results indicate that the interaction between UV and t is significant, which is also presented in Table 4.

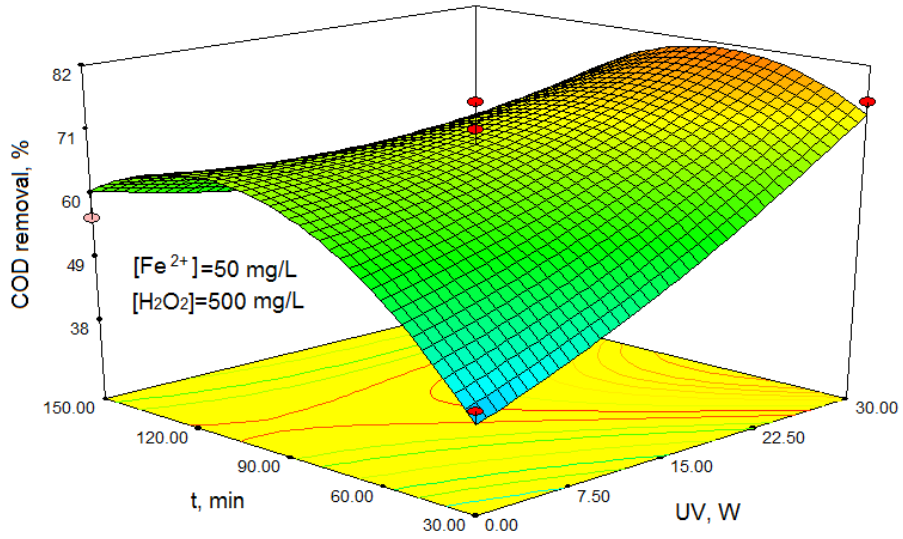

Fig. 5. Three-dimensional plot of the COD removal by ultraviolet intensity and treatment time ($[Fe^{2+}] = 50$ mg/l, $[H_2O_2] = 500$ mg/l, $T = 25$ ℃, $P = 1$ atm, and stirring speed of 350 rpm)

Fig. 6 shows a three-dimensional plot of the COD removal by ferrous concentration and hydrogen peroxide concentration when applying $UV = 15$ W with a treatment time of $t = 90$ min. As presented in this figure, at high concentrations of Fe (II) and low concentrations of hydrogen peroxide ($[Fe^{2+}] = 90$ mg/l and $[H_2O_2] = 100$ mg/l) the COD removal rate was at the highest level.

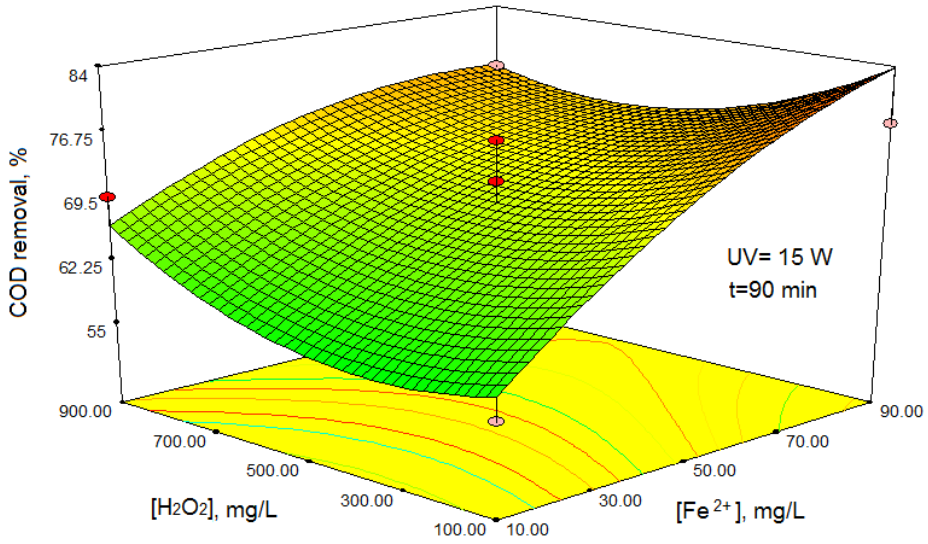

Fig. 6. Three-dimensional plot of the COD removal by ferrous concentration and hydrogen peroxide concentration ($UV = 15$ W, $t = 90$ min, $T = 25$ ℃, $P = 1$ atm, and stirring speed of 350 rpm)

Moreover, Fig. 7 shows the three-dimensional plot of the COD removal by the concentration of ferrous and treatment time when applying $UV = 15$ W and $[H_2O_2] = 500$ mg/l. As seen in, the COD removal rate was higher at moderate treatment times in all $[Fe^{2+}]$ values. As previously mentioned, the decreased level of the COD removal rate can be attributed to the side reactions.

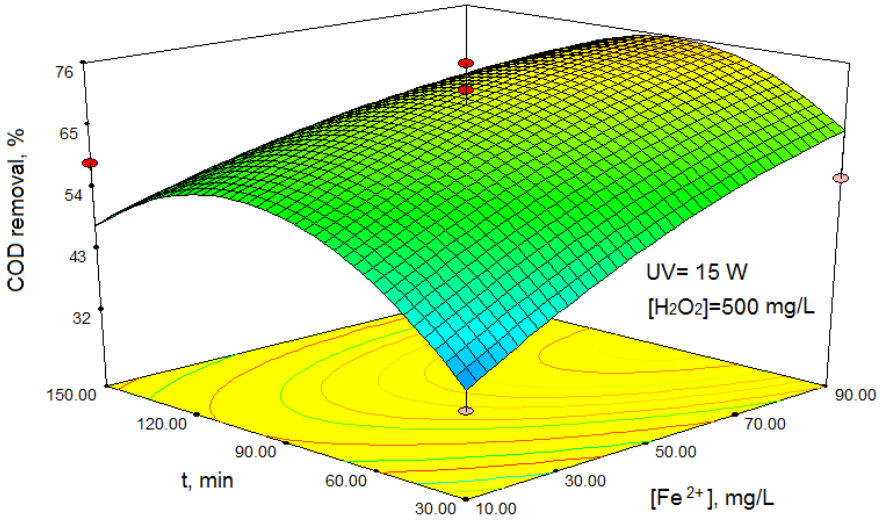

Fig. 7. Three-dimensional plot of the COD removal by ferrous concentration and treatment time ($UV = 15$ W, $[H_2O_2] = 500$ mg/l, $T = 25$ ℃, $P = 1$ atm, and stirring speed of 350 rpm)

Fig. 8 shows a three-dimensional plot of the COD removal by hydrogen peroxide concentration and treatment time when applying $UV = 15$ W and $[Fe^{2+}] = 90$ mg/l. As clearly shown in this figure, at low concentrations of hydrogen peroxide, when the treatment time is 150 min, the COD removal rate was at the highest level. Furthermore, when the treatment time is short, it can be compensated by increasing the concentration of hydrogen peroxide. However, when the experiment was conducted under a longer treatment time and using higher concentrations of hydrogen peroxide, the COD removal rate was low that can be attributed to the side reactions occurring over time. It reflects the strong interaction between the parameters of hydrogen peroxide concentration and treatment time (Table 4).

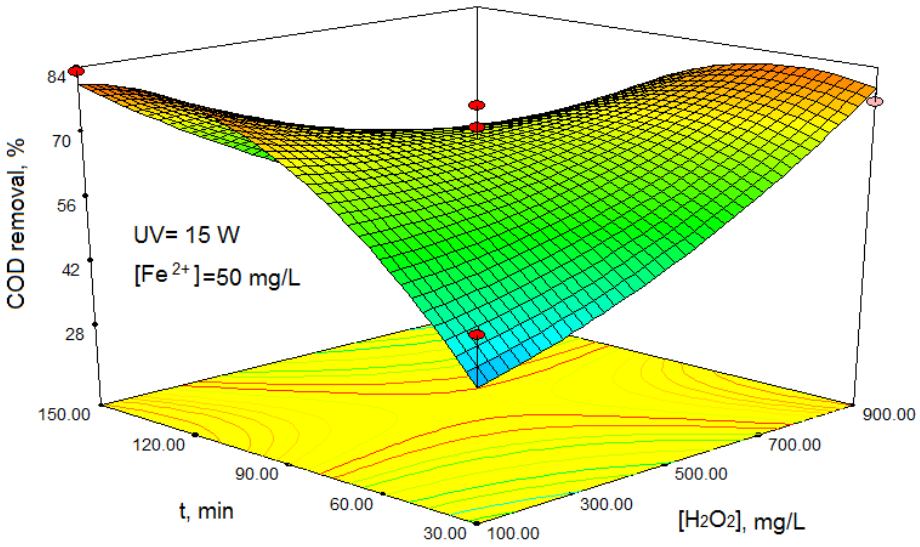

Fig. 8. Three-dimensional plot of the COD removal by hydrogen peroxide concentration and treatment time ($UV = 15$ W, $[Fe^{2+}] = 50$ mg/l, $T = 25$ ℃, $P = 1$ atm, and stirring speed of 350 rpm)

Determination of optimal conditions

As shown in Figs. 3 to 8, the high percentage of COD removal can be achieved in different conditions. The intensity of UV light can only be 0, 15, and 30 W, depending on the lamps used. Therefore, the optimal condition was determined by utilizing these three values for setting UV light intensity. Using Design Expert 7.0.0 software, the values of the other variables were achieved in three UV light intensities to maximize the COD removal. These optimal values, along with the percentage of the COD removal are shown in Table 5.

As shown in Table 5, when the intensity of the UV lamp is zero (Fenton process), the best COD removal rate obtained by the proposed model was 96.61%. In that condition, the concentration of iron ion was 82.9 mg/l, the concentration of the hydrogen peroxide was 119.9 mg/l, and the treatment time was 135.9 min. However, when the intensity of the UV lamp was 30 W (photo-Fenton process), the best COD removal rate obtained by the proposed model was 92.82%. In that condition, the concentration of ferrous was 35.1 mg/l, the concentration of hydrogen peroxide was 110.2 mg/l, and the treatment time was 92.8 min. It was observed that the photo-Fenton process (UV light intensity of 30 watts) had a condition that was similar to that of the Fenton process, however, the treatment time was 43 min shorter.

Table 5. Optimal parameters and COD removal

Optimal parameters				$COD_{rem.}$,%
***UV*, W**	**[Fe^{2+}], mg/l**	**[H_2O_2], mg/l**	***t*, min**	
0	82.9	119.9	135.9	96.61
15	89.9	100.3	116.5	87.84
30	35.1	110.2	92.8	92.82

Conclusion

In this study, based on the results of the Box-Behnken experimental design method, the amount of COD in the wastewater of Kermanshah oil refinery decreased using Fenton and photo-Fenton processes. The effects of UV light intensity, iron ion concentration, hydrogen peroxide concentration, and treatment time on industrial wastewater COD removal were studied. The statistical analysis of the model was performed and it was found that the model had a satisfactory performance in predicting the percentage of the COD removal. The effects of variables on the removal of COD were investigated, and a quadratic polynomial model was

fitted to the empirical data. In the Fenton process ($UV = 0$), the optimal concentration of iron ions was 89.2 mg/l, the concentration of hydrogen peroxide was 119.9 mg/l, and the treatment time was 135.9 min. However, in the photo-Fenton process at a UV intensity of 30 W, the optimal value of $[Fe^{2+}]$, $[H_2O_2]$, and treatment time was 35.1 mg/l, 110.2 mg/l, and 92.8 min, respectively. The photo-Fenton process has the advantage of reducing the chemicals and the treatment time, but its energy consumption is high. Energy consumption can be reduced by using sunlight instead of artificial UV light.

Acknowledgment

The authors would like to acknowledge the financial support of the Kermanshah University of Technology for this research under grant number S/P/T/1124.

Nomenclatures

ANOVA	Analysis of variance
AOP	Advanced oxidation process
b_0	Constant number
b_i	Slope of the variable
b_{ii}	Second-order of the input variable x_i
b_{ij}	Linear interaction between the input variables x_i and x_j
BOD	Biological oxygen demand (mg/l)
COD	Chemical oxygen demand (mg/l)
$[COD]_0$	COD value at the start of the reaction (mg/l)
[COD]	COD value at the time of the process (mg/l)
$COD_{rem.}$	Removal of COD (%)
DF	Degree of freedom
DO	Dissolved oxygen
$[Fe^{2+}]$	Ferrous ion concentration (mg/l)
H_2O_2	Hydrogen peroxide concentration (mg/l)
k	Rate constant of reaction (mol/l.s)
MS	Mean of square
Res.	Response variable
RSM	Response surface method
SS	Sum of square
t	Treatment time (min)
TDS	Total dissolved solids (mg/l)
TSS	Total suspended solid (mg/l)
UV	Ultraviolet light intensity (W)

References

[1] Bokare AD, Choi W. Review of iron-free Fenton-like systems for activating H2O2 in advanced oxidation processes. Journal of Hazardous Materials. 2014 Jun 30;275:121-35.

[2] Cortez S, Teixeira P, Oliveira R, Mota M. Fenton's oxidation as post-treatment of a mature municipal landfill leachate.

[3] Iqbal M, Bhatti IA. Re-utilization option of industrial wastewater treated by advanced oxidation process. Pakistan Journal of Agriculture Sciences. 2014 Dec 1;51(4):1141-7.

[4] Chiou CS. Application of steel waste with UV/H2O2 to mineralize 2-naphthalenesulfonate in aqueous solution. Separation and purification technology. 2007 May 15;55(1):110-6.

[5] Primo O, Rivero MJ, Ortiz I. Photo-Fenton process as an efficient alternative to the treatment of landfill leachates. Journal of hazardous materials. 2008 May 1;153(1-2):834-42.
[6] Riga A, Soutsas K, Ntampegliotis K, Karayannis V, Papapolymerou G. Effect of system parameters and of inorganic salts on the decolorization and degradation of Procion H-exl dyes. Comparison of H2O2/UV, Fenton, UV/Fenton, TiO2/UV and TiO2/UV/H2O2 processes. Desalination. 2007 Jun 10;211(1-3):72-86.
[7] Bautista P, Mohedano AF, Casas JA, Zazo JA, Rodriguez JJ. An overview of the application of Fenton oxidation to industrial wastewaters treatment. Journal of Chemical Technology & Biotechnology: International Research in Process, Environmental & Clean Technology. 2008 Oct;83(10):1323-38.
[8] Meriç S, Kaptan D, Ölmez T. Color and COD removal from wastewater containing Reactive Black 5 using Fenton's oxidation process. Chemosphere. 2004 Jan 1;54(3):435-41.
[9] Arslan-Alaton I, Tureli G, Olmez-Hanci T. Treatment of azo dye production wastewaters using Photo-Fenton-like advanced oxidation processes: Optimization by response surface methodology. Journal of photochemistry and Photobiology A: Chemistry. 2009 Feb 25;202(2-3):142-53.
[10] Aziz AA, Daud WM. Oxidative mineralisation of petroleum refinery effluent using Fenton-like process. Chemical engineering research and design. 2012 Feb 1;90(2):298-307.
[11] Hermosilla D, Cortijo M, Huang CP. Optimizing the treatment of landfill leachate by conventional Fenton and photo-Fenton processes. Science of the Total Environment. 2009 May 15;407(11):3473-81.
[12] Rezaei R, Mohadesi M, Moradi GR. Optimization of biodiesel production using waste mussel shell catalyst. Fuel. 2013 Jul 1;109:534-41.
[13] Ferreira SC, Bruns RE, Ferreira HS, Matos GD, David JM, Brandao GC, da Silva EP, Portugal LA, Dos Reis PS, Souza AS, Dos Santos WN. Box-Behnken design: an alternative for the optimization of analytical methods. Analytica chimica acta. 2007 Aug 10;597(2):179-86.
[14] Federation WE, American Public Health Association. Standard methods for the examination of water and wastewater. American Public Health Association (APHA): Washington, DC, USA. 2005.
[15] El-sousy K. Elimination of organic pollutants using supported catalysts with hydrogen peroxide.
[16] Ferreira SC, Bruns RE, Ferreira HS, Matos GD, David JM, Brandao GC, da Silva EP, Portugal LA, Dos Reis PS, Souza AS, Dos Santos WN. Box-Behnken design: an alternative for the optimization of analytical methods. Analytica chimica acta. 2007 Aug 10;597(2):179-86.
[17] Montgomery DC. Design and analysis of experiments. John Wiley & Sons. Inc., New York. 2001;1997:200-1.
[18] Çatalkaya EÇ, Şengül F. Application of Box–Wilson experimental design method for the photodegradation of bakery's yeast industry with UV/H2O2 and UV/H2O2/Fe (II) process. Journal of hazardous materials. 2006 Feb 6;128(2-3):201-7.
[19] Liou MJ, Lu MC, Chen JN. Oxidation of explosives by Fenton and photo-Fenton processes. Water Research. 2003 Jul 1;37(13):3172-9.
[20] Nitoi I, Oncescu T, Oancea P. Mechanism and kinetic study for the degradation of lindane by photo-Fenton process. Journal of Industrial and Engineering Chemistry. 2013 Jan 25;19(1):305-9.